

## **Chapter 4**

### **Experimental model and model verification**

#### **(Laser radar and laser tracker through window test to measure targets apparent position)**

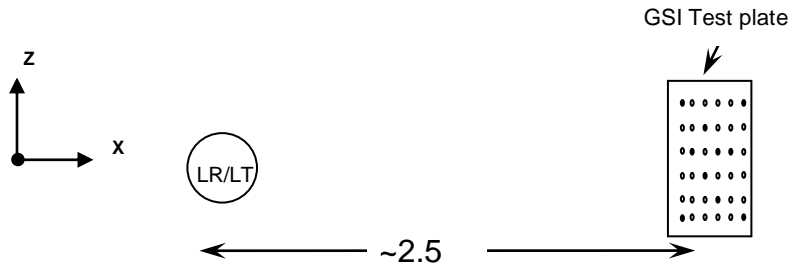
This chapter makes use of the three previous chapters. The first 2 chapters have guided our understanding on how the laser radar and laser tracker work, so that at the end of this chapter, when we are interpreting the results, these can be considered accurate. Chapter 3 explicates the physical effect of a plane parallel plate by providing the model that indicates how much a window can apparently shift an image; in that chapter we also showed the Zemax numerical model, which we will use to compare with the experimental model developed in this chapter.

Therefore, this chapter presents the measurements collected with the LR and the LT when observing 11 targets with and without a window. The LR measured an array of 11 tooling balls (TB) and 11 holes, and the LT measured an array of 11 spherically mounted reflectors (SMR), where the TB and SMR were interchangeable in 11 magnetic nests that went over previously punctured holes on the test plate.

#### **4.1 Experimental test setup**

The first test setup consisted of the laser radar, laser tracker and the GSI test plate approximately 2.5 meters apart to measure the targets located on the plate, such that the line of sight between the laser beam emitted by the instruments and the middle of the plate lied

in a plane roughly perpendicular to gravity as shown in Figure 17. The data discussed in Chapter 1 was collected using this setup but had a different use, explained in that chapter.



**Figure**

**17:**

**Initial test setup without window (side view).**

We arranged another setup with a window mount between the instrument and the test plate such that the measurement beam from the LR and LT to the plate would propagate through the window, this setup is illustrated in Figure 18. We roughly leveled the window mount so that the window normal would be parallel to the instrument's measuring beam and perpendicular to gravity. We document and indicated the arrangement of the TB and SMR on the test plate in Figure 19. The distance between the instruments and the window was determined by the physical constraints of the facilities. The original test setup has a large window mount which constrains the distance of the instruments to the window. Ideally the instruments should only be a few centimeters away from the window, because the closer the instrument is to the window, the wider the range of sight will the instruments have. In this case, 40 cm was the minimum distance determined by the setup.

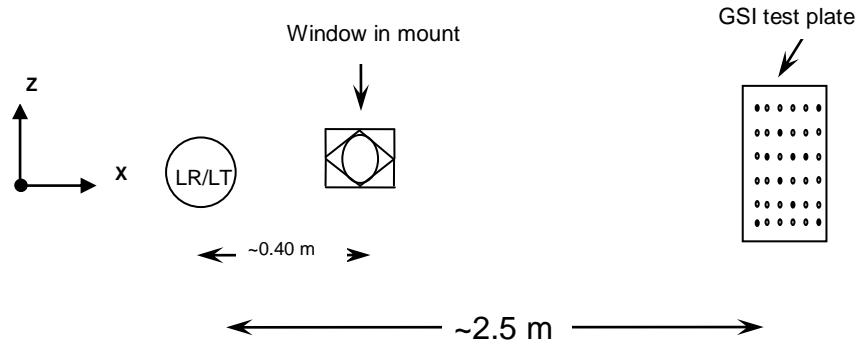


**Figure 18:** Test setup with window installed (side view).

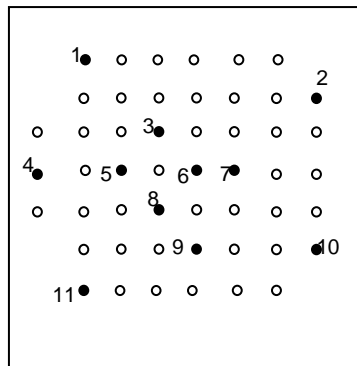


**Figure 19:** GSI plate with the target mounts labeled locations.

Once the setup was ready, we conducted 3 different tests. The first one with 11 tooling ball locations (11 mounts) and the LR, the second one with 11 SMR locations (11 mounts) and the LT, and finally, the last test with 11 holes from the GSI plate and the LR. All the data was collected through Spatial Analyzer.

#### 4.2 Methodology for the experimental setup for data verification

1. We run the LR and LT start-up procedure, each one separately. Before running the laser radar procedure we had to perform calibration tests. These tests had to be done prior to data collection, because if performed after or during, the instruments reference system could

change, therefore changing the measured results. These calibration tests were: linearization, self test, flip test (which requires measuring a tooling ball) and LO separation test (which requires measuring a tooling ball at least 8 meters away). All of these are located in the test tab in the SA interface module.

When we run the laser tracker procedure, we set it to be in ADM mode and then we released the motors so that the instruments head could be manually positioned to then search and lock on the selected SMR. The seed distance (which had to be measured) and search radius were required dimensions for the LT interface. All of these options were found on the ADM drive button in the SA interface module.

2. We arranged the setup so that it looked like Figure 17.
3. We distributed the mounts and targets on the GSI plate as shown in Figure 19 when we measured the tooling balls and SMR. We left the GSI plate bare when we measured the holes.
4. In spatial analyzer we created a new point group called “No window1”.
5. We measured the position of each tooling ball and hole with the LR, and of each SMR with the LT. We cycled through the sets of targets a total of 10 times. The targets were measured in the order shown in Figure 19. It is important to note that when we measured the holes with the LR, we used the hole feature. In this case, we had to indicate the hole diameter and chamfer size.
6. We placed scotch tape on the window, as shown in Figure 20. Four isosceles triangle shaped pieces of tape of approximately 4 cm of surface area. The tape was used to measure the location of the window with the LR. It is important to know the windows location so that the window normal can be located and we can measure the angle of incidence of the measuring beam, measured from the window normal. We care about the angle of incidence

of the beam so that we can correlate the apparent target shift to a certain angle of incidence of the measuring beam in the final results.

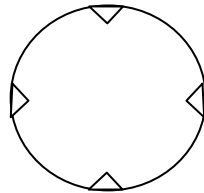


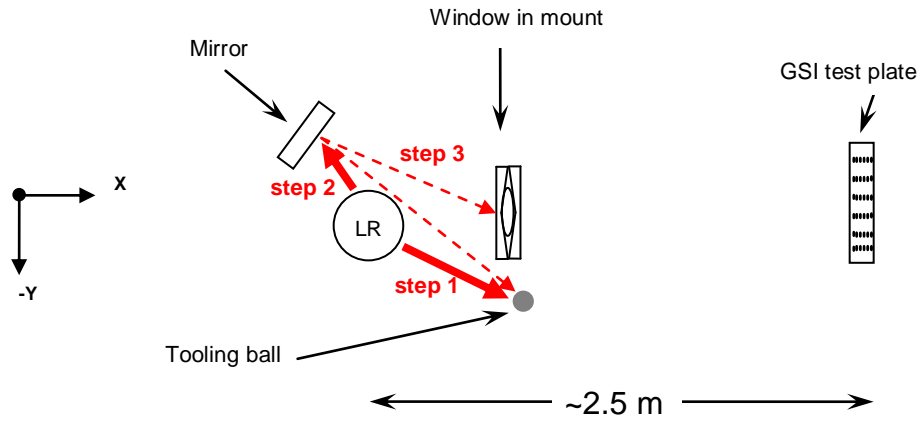
**Figure 20: Window with scotch tape.**

7. We arranged the setup so that it looked like Figure 18. We installed the window on the window mount and aligned it such that the normal to the window was roughly parallel to the instruments measurement beam. It was important for us to keep in mind the orientation of the window. To indicate it on the window we used a marker, so that it would remain constant through all 3 different tests, which were mentioned at the end of section 4.1.
8. We measured the location of the window by measuring its front surface (first side from instrument to target plate).
  - When we used the LT, we scanned a retroreflector across the window's front surface.
  - When we used the LR, we arranged a setup similar to that shown in Figure 21. It was important that the mirror reflected off the window and the tooling ball, because the mirror allowed us to measure the position of the window. The mirror was required because the LR is not capable of focusing, and therefore measuring, on anything located one meter away from its head. By looking at Figure 18, we notice that the window is approximately 40 cm away from the instrument, by using the mirror, the LR was be able to measure the location of the window through the mirrors reflection, as a result of using the 'reflect all

measurements' feature on the SA laser radar interface. We took the following steps to complete the measurement:

- 1) Once we had the setup shown in Figure 21, we clicked on the mirror icon of the SA interface and measured the tooling ball directly from the instrument (step 1 in Figure 21).
- 2) We immediately measured the tooling ball's reflection, by pointing the LR at the mirror (step 2 in Figure 21).
- 3) By using the mirror feature on spatial analyzer, we created the mirror plane, detected by the instrument, and the mirror definition points.
- 4) We checked the 'reflect all measurements' box of the SA interface. This feature used the mirror plane to reflect off it the pieces of tape.
- 5) We scanned the reflected pieces of tape, using a vision scan box of 18 x 18mm with a 2mm line spacing, each of the pieces of the window tape: top, bottom, left and right, and labeled them after their location. These points were saved as point clouds and required to be transformed to point groups during analysis (step 3 in Figure 21).
- 6) When the window scans were done, we checked again 'reflect all measurements' to stop measuring through the mirror's reflection.
9. We created a new point group called "Window1" and measured the position of each target (tooling balls, holes and SMR) with the LR/LT, cycling through the set of targets a total of 10 times.

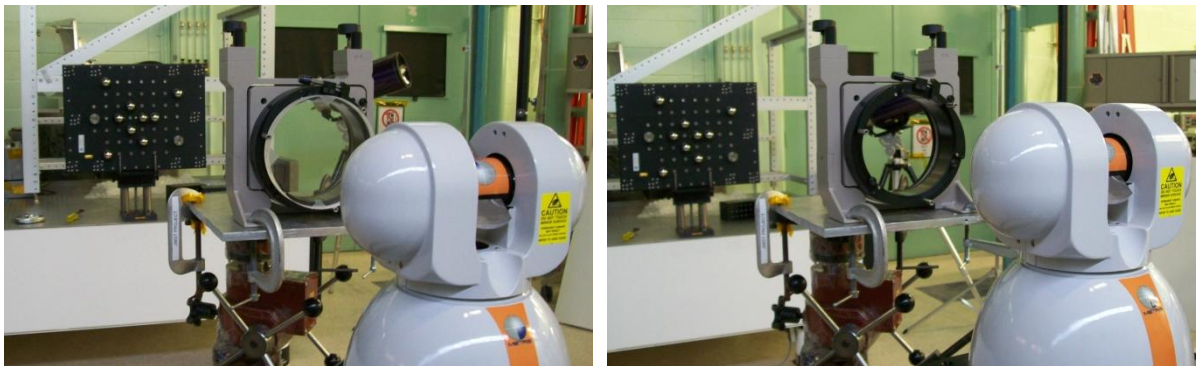
Images from the real setups, with (a) and without a window (b) are shown in Figure 22.



**21:**

**Figure**  
**Mirror**

**setup for measuring the window with the LR (top view).**



**a)**

**b)**

**Figure 22: Side view of the real experimental setup.**

**a) With a window and, b) Without a window.**

### **4.3 Data analysis and model comparison**

We used the data collected during steps 5 and 9 of section 4.2 to calculate the apparent shifts for both axial and transverse directions. The axial direction is along the optical path length (OPL); from the instrument, through the window towards the plate. The transverse direction is the height of the target on the target plate plane, starting at a position normal to

the window. Figure 23 shows the axial direction as the x axis and the transverse direction as the z axis. The axis labeling was predetermined by spatial analyzer and we simply continued to use the same nomenclature.

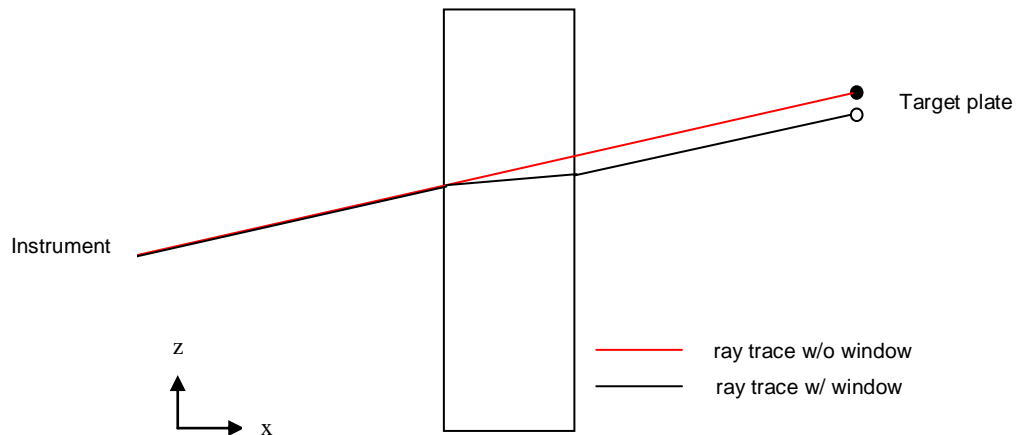


**Figure 23: Axial (x axis) and transverse (z axis) directions.**

To calculate the measured transverse and axial shifts, we required the average location of the observed targets with and without a window.

We also had to visually scan all the data points to verify the correct labeling of the measurements and to determine possible bad points to eliminate them. When we observed the data points measured with the laser radar, it was visually clear that the first measured point out of the 10 measurements per cycle was most of the times (~90%) separated from the rest of the data,  $\sim 10\sigma$ . Every time this occurred, we considered it to be a bad point and that data did not contribute to the average calculation of the target's location nor its error propagation. Figure 24 shows an example of what a bad point looked like in spatial analyzer. A possible explanation for this effect could be a combination of 2 actions done by the user. The first one could be the use of the autofocus and the second, the double click dragging function. When the laser radar measured for the first time, we auto focused the



beam on the object to be measured to verify a clear return at each target location. We did this for the first measured cycle. For the 9 cycles after that, we used the double right click dragging function and we did not make use of the autofocus function anymore. The dragging function allowed us to double right click on a location previously measured in spatial analyzer and that would drag the laser beam to that specific location again. By doing this, the operator does not have to visually find the target again, making the data collection run much faster. Since we did not use autofocus function when we used the drag function, it is possible that the first cycle was measured slightly different than the other nine cycles, this could explain the separation of the first measured cycle from the rest of the measured points, as shown in the following figure.

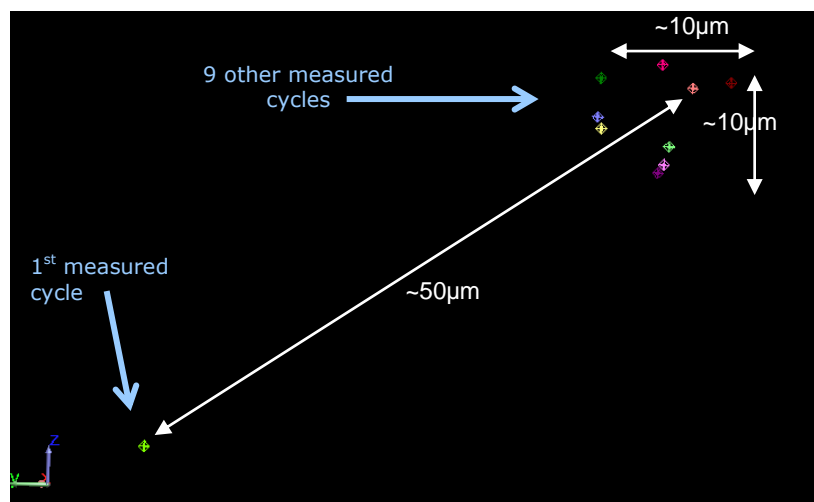


**Figure 24: Example of a bad point in green.**

Once we identified the bad points and calculated the average target locations, we had to determine the error associated with each measured target. To find out this result we calculated the error uncertainty for each target location by using the error propagation equation,

(9)

$$\sigma_x^2 \approx \sigma_u^2 \left( \frac{\partial x}{\partial u} \right)^2 + \sigma_v^2 \left( \frac{\partial x}{\partial v} \right)^2 + \dots,$$

where  $x = f(u, v, \dots)$ . We calculated the uncertainty values for each target using excel and these are shown in the axial and transverse shift plots (Figures 25 through 30) as error bars for the dependant variable.

We measured the incident angle, which is the independent variable associated with each target location with respect to the window normal by using spatial analyzer. To measure it, we had to construct a series of lines from each target average location to the frame origin and an additional line normal to the window plane. We had measured the window surface location in order to obtain its normal vector. The measurement in degrees between the target line and the window normal is the value indicated in the axial and transverse shift plots as the independent variable.

Since we had 3 different test setups, as we mentioned at the end of section 4.1, each incident angle value slightly varied from setup to setup, however, they were correlated, as we can see in the plots. These plots show the axial and transverse measured shifts for each setup. The 1<sup>st</sup> setup used tooling balls measured with the laser radar, the 2<sup>nd</sup> used SMR observed with the laser tracker, finally the 3<sup>rd</sup> setup measured holes from the GSI test plate with the laser radar again. Furthermore, each plot also shows, besides the experimental model, the Zemax numerical simulation explained in section 3.3 to compare it to the measured data.

Every plot shows the apparent shift created by the presence of the window in the experiment. To determine the plotted shift value, in both axial and transverse directions, we subtracted the measured value without a window to that measured with a window.

Before discussing the experimental to theoretical comparison we will mention that when measuring SMR with a laser tracker it is important to keep in mind that these targets have a small offset associated with their fabrication configuration, like we mentioned in Chapter 1. The apex of the corner cube does not agree with the center of the sphere, because it is shifted a few microns towards the surface of the sphere (see Figure 4). This disagreement creates an offset between the TB data and the SMR data, because the laser radar does measure the location of the center of the TB but the LT measures the apex location, not the center. The offset is not important when all the measurements are collected with the same instrument and same targets, but when measuring with different instruments, like this thesis, it is important to keep it in mind.

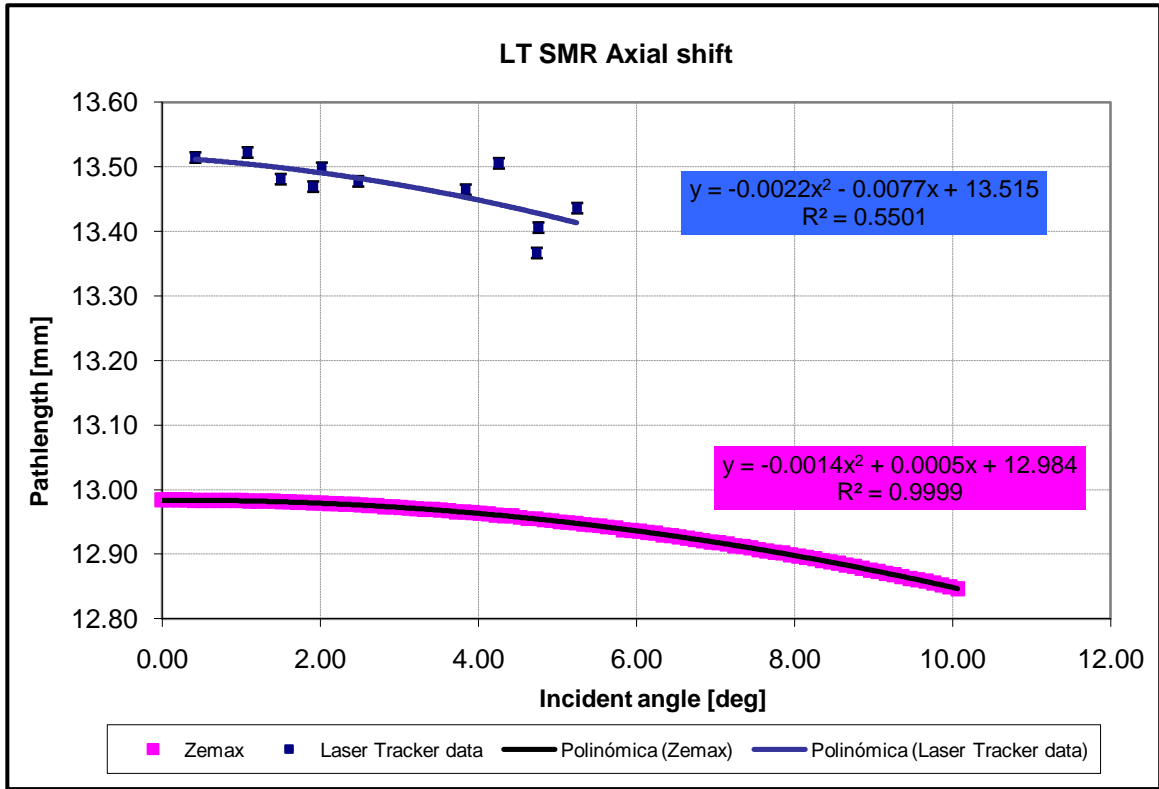
Another thing that we took into account when we measured the SMR with the laser tracker was the correspondence between the number of mounts and the number of SMR. During the measurement we had 11 mounts, as indicated in Figure 3, but only 1 SMR. This meant that we had to manually displace the target to every location every cycle. Since the target mounts are magnetic, when the SMR was placed on the mount, the target was immediately attracted to it; so even though we tried to locate the target as gently as possible on the test plate mount to avoid making the plate vibrate, we did not always accomplish this. However, every cycle, we had to move the target to all different locations, the systematic error introduced by the possible plate motion was taken into account in the standard deviation of the data at every location.

When comparing the Zemax numerical simulation with the measured data, we used the same notation in all the plots. The blue line represents the fit of the measured points and the pink set of points represents the Zemax simulation. The equation for each serie has the same color as the fit line.

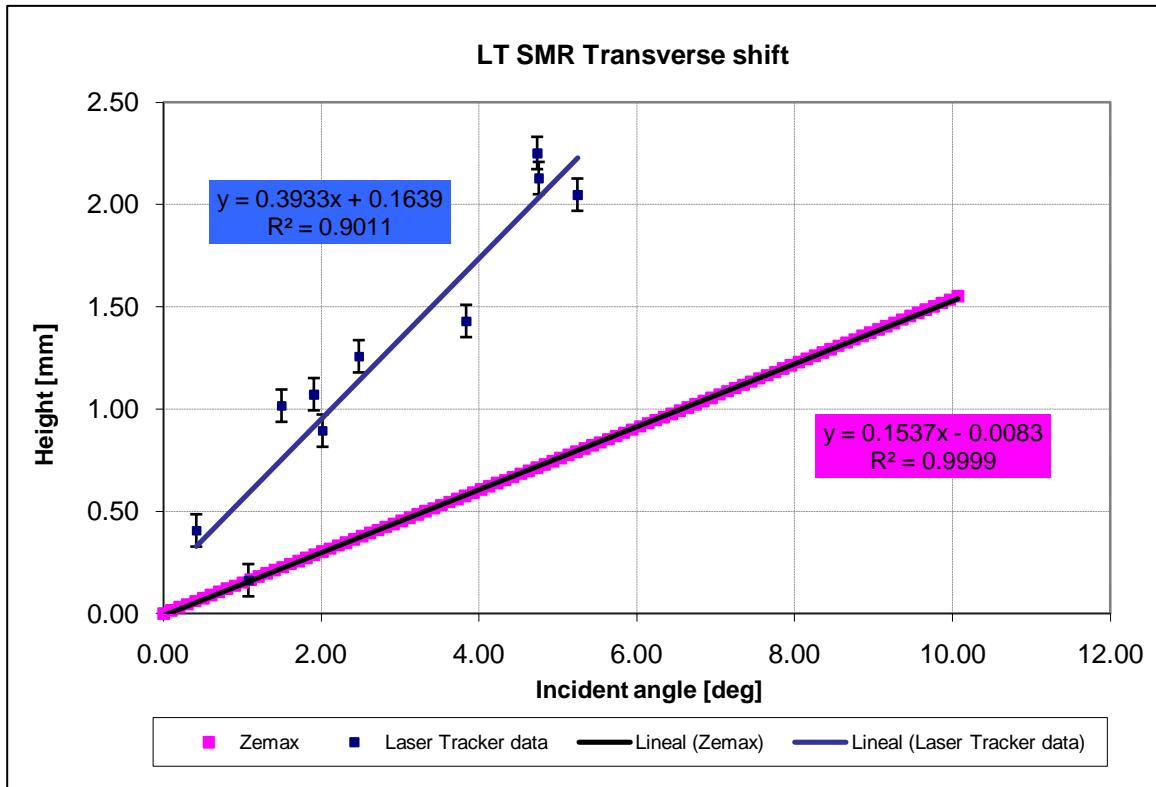
Figure 25 shows the window to no window apparent target shift in the x axis measured with the laser tracker. Let us remember that as shown in Figure 23, the x axis is along the optical path length that goes from the instrument, through the window, towards the test plate and we call it the axial direction.

Figure 26 shows the window to no window transverse shift (in the z axis) measured with the laser tracker. The measurements lie on the test plate plane and the origin is located where the window normal vector intersects the plate plane. The measurement begins at the center, which is close to the plate center of mass and ends at the target location.

The error bars of the shifts on both figures were calculated with the error propagation formula (equation (9)). We can observe that Figure 26 has larger errors than Figure 25. Since the optical path length (axial direction) was measured directly by the instrument and was the value of the x axis, when we calculated the error propagation of the axial shift there was less error propagated in this case than when we calculated the error associated with the transverse shift, because the height value was not directly measured by the instrument, but was determined by the values of both y and z axis, causing the calculated error to be larger in the transverse shift plots.



**Figure 25: Laser tracker axial shift comparison plot.**



**Figure 26: Laser tracker transverse shift comparison plot.**

Figures 25 and 26 aside from showing the fit equations, also show the determination coefficient  $R^2$ , which values ranges from 0 to 1. This coefficient is a statistic that denotes strength between 2 variables. The closer the value is to 1, the stronger the relationship among them is. A reasonably good coefficient would be 0.8.

For figures 25 and 26, the Zemax numerical simulation show a high determination coefficient, this indicates that the equation for that set of points is very faithful to the actual data points. On the other hand for the experimental model in figure 25, the determination coefficient is 0.5, a low coefficient, which indicates that the data is dispersed and that the equation for that polynomial fit is not very accurate.

Figures 25 and 26 also show a disagreement between the measured data and the modeled data, even when considering the error bars, the difference is simply too big. There are several reasons why we believe this occurred, we will discuss them later in the conclusions.

Figures 27 and 28 illustrate the window to no window axial and transverse shifts respectively for the laser radar when measuring tolling balls. Figure 27 shows the comparison of the experimental axial measured shift compared with the Zemax simulation shift; figure 28 shows both data again but this time in the transverse direction. Once again, we notice the same effect on the error bars of the measured data and we believe that similar to the LT data, the LR data shows again a larger propagated error when measuring the transverse shift. Also, both data series, measured and simulated by Zemax, disagree again, having a completely different slope in the linear case with the transverse shift, and for the axial shift, a difference of up to half of millimeter of depth. Another thing that repeats in these plots is the determination coefficient, which is high for the Zemax simulation equations, indicating high correlation between the variables; however, for the experimental

results the coefficient is low, indicating, that the equations are not exact and can easily change by adding or taking data points.

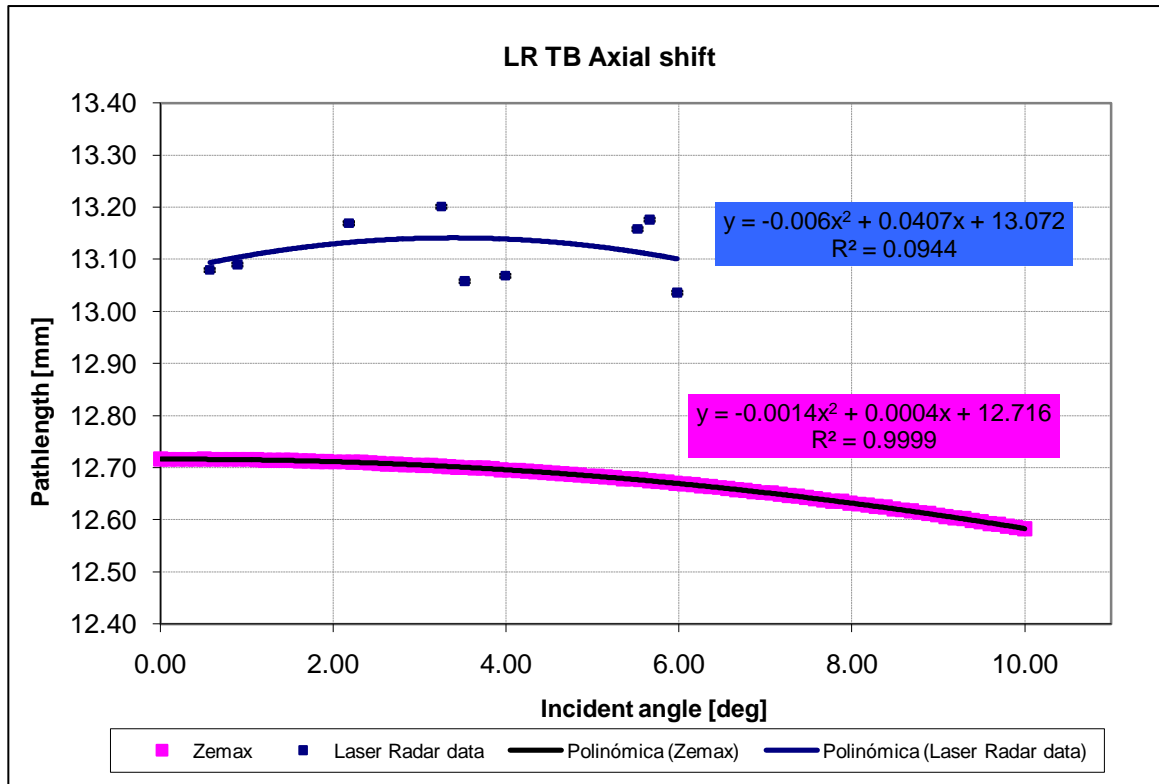


**Figure 27: Laser radar (tooling ball targets) axial shift comparison plot.**

Figures 29 and 30 show the window to no window axial and transverse shifts respectively for the LR data measuring the hole feature. Yet again, like it occurred in the previous sets of plots there is a significant difference in the error bar size in the transverse shift plot compared to the axial shift plot, caused by the data source: for the axial shift, we calculated the propagating error after calculating the difference directly from the x axis measurement, along the optical path length; for the transverse case we calculated the final propagating error after calculating the target height from the measured data which has its own error,

then, we calculated the difference (window to no window) to finally calculate the error. The additional calculation made the error increase approximately 40 times.

Just as we observed in figures 25, 26, 27 and 28, figures 29 and 30 present again the determination coefficient,  $R^2$ , under the fit equation in every plot. For figure 29, the experimental data indicates a coefficient value of almost 0.7, which is better than the others shown when measuring the axial shift, this could be have been caused by the instrument measuring a different target, a hole feature. But even when we have a 0.7 determination coefficient, it is still considered low. For figure 30 the coefficient value is similar to those shown in the previous transverse shift plots, 0.5, which as we mentioned before, indicates a low accuracy model due to the dispersed data.

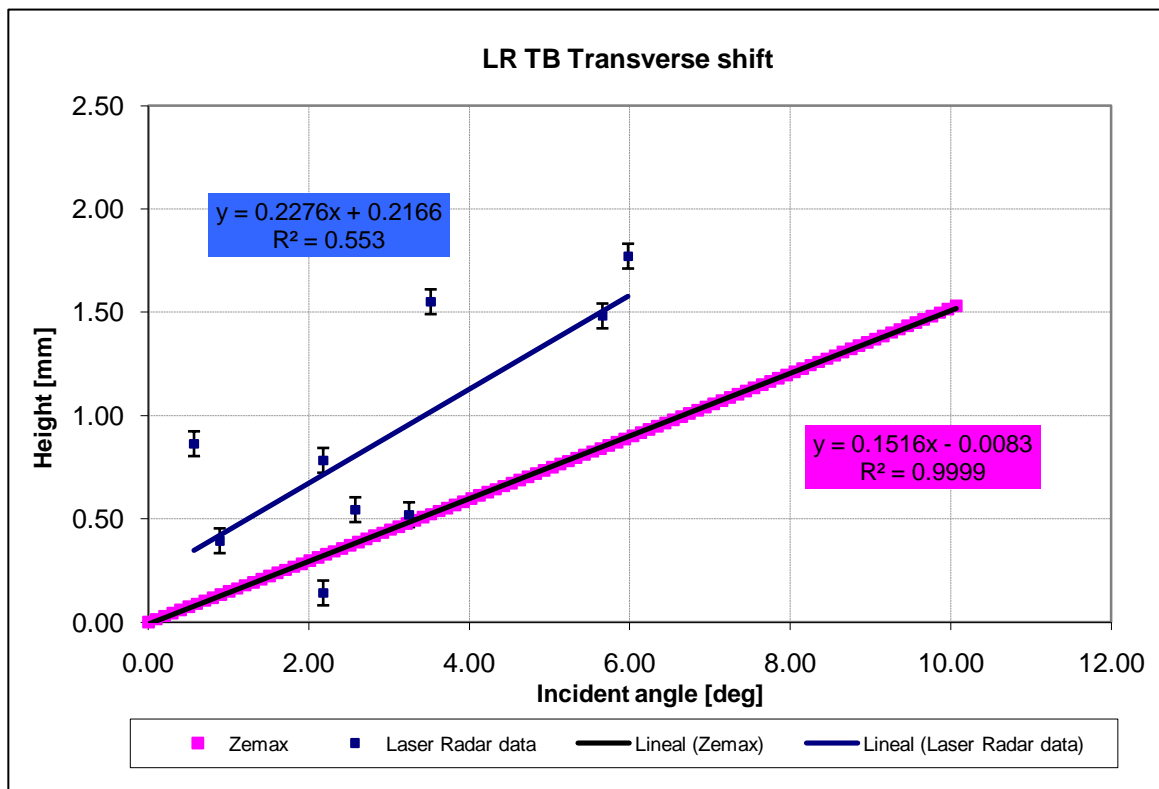


**Figure 28: Laser radar (tooling ball targets) transverse shift comparison plot.**



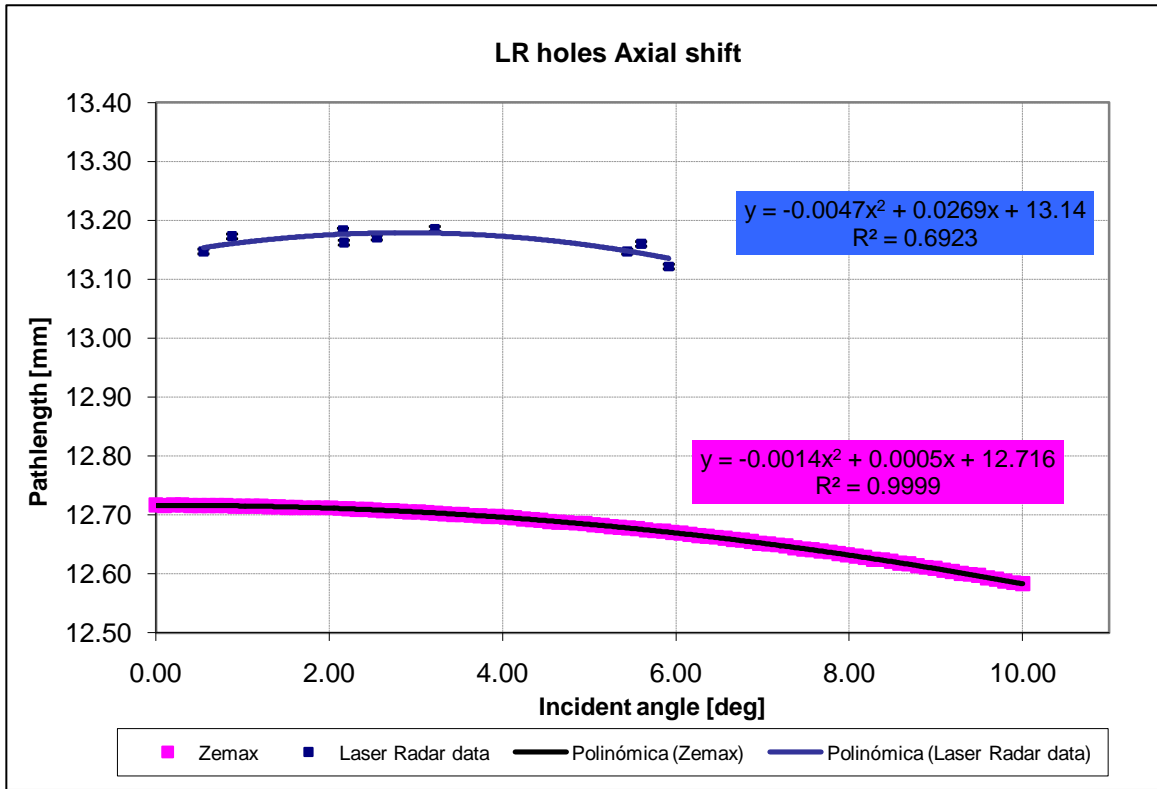


**Figure 29: Laser radar (hole targets) axial shift comparison plot.**

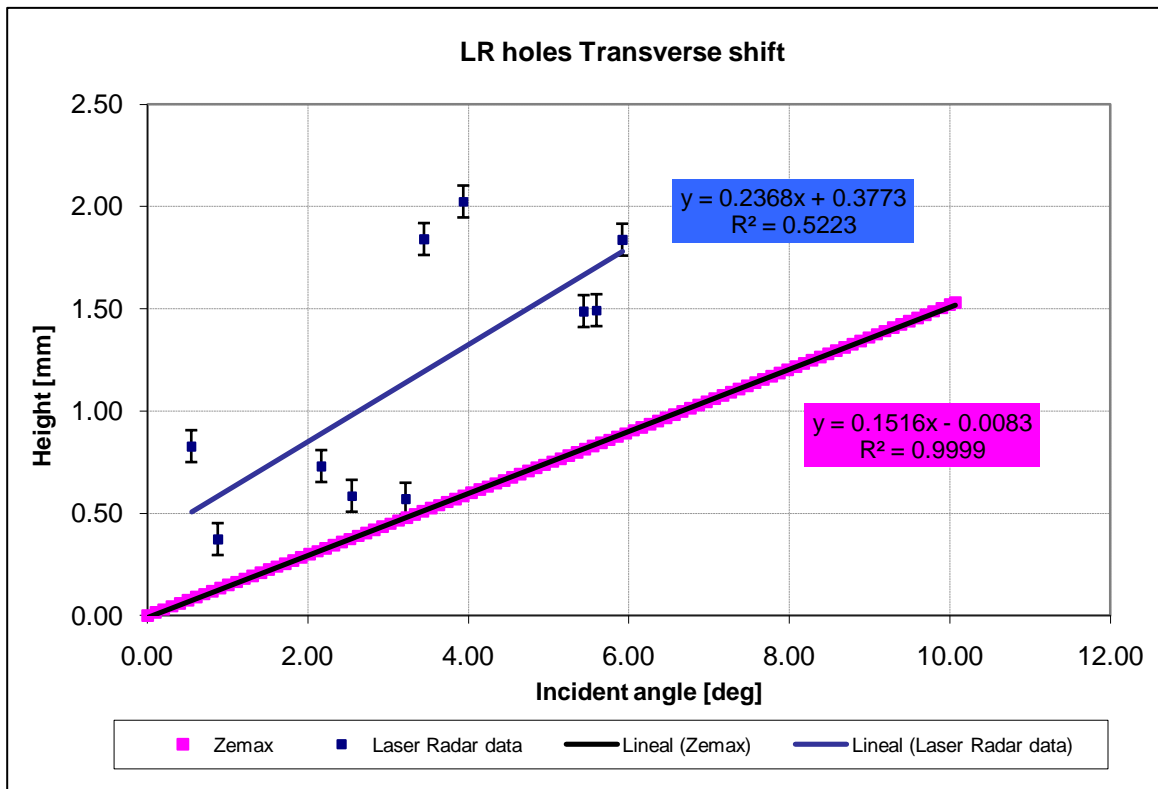


**Figure 30: Laser radar (hole targets) transverse shift comparison plot.**